

Full Length Research Paper

# Effective rigid perfectly plastic models to predict deflection and residual velocity of post local failure motion of impulsively loaded circular plates

Asghar Zajkani<sup>1\*</sup>, Morteza Nikooyiha<sup>1</sup>, Abolfazl Darvizeh<sup>2</sup> and Mansour Darvizeh<sup>1</sup>

<sup>1</sup>Department of Mechanical Engineering, Engineering Faculty, University of Guilan, P. O. Box 3756, Rasht, Iran.

<sup>2</sup>Department of Mechanical Engineering, Engineering Faculty, Islamic Azad University of Bandar Anzali, Anzali, Iran.

Accepted 11 March, 2013

Two deformation models are proposed for clamped circular plates undergoing pulse loadings. By these models, behaviors of plate are studied effectively for the situations before and after local failure. In the first model, it is assumed that impulsive load is uniformly distributed and final deformation is of a spherical dome shape. In order to analyze this model, it assumed that under the shock wave, the mechanism of deformation is represented by a multi-peripheral stationary hinge scheme. In the second model, the final shape is considered to have a conical shape represented by a single peripheral plastic moving hinge. In this part, an alternate deformation model is proposed and the final shape is induced by transverse and radial motion of the plastic hinge. For each model, the deformation and motion after severance of the plate (post local failure) will be analyzed. Calculated plastic energies dissipated in deformation process, energy absorbed in boundaries during failure, residual kinetic energy and velocity after local failure are evaluated and discussed. Computed results show good agreement between our approaches and experimental data; better than that obtained with other models.

**Key words:** Impulsive load, shear local failure, plastic hinge, rigid perfectly plastic, residual kinetic energy.

## INTRODUCTION

The plate structures are important in many applications such as; aerospace industry, and designing and fabrication of submarines, ships, bridges and vessels. For example; hull plates with small curvatures are welded together and supported by mechanical parts. The plates between these parts can be considered by a flat sheet. In some situations, the plate structures may be subjected to impacts and shock waves. So, analysis of their behaviors is remarkable for engineering safety designers. Enhancement of pressure pulse increases probability of rupture occurrence and or tearing of plate. Loading consequences and failure expectation of circular plates

under impulsive loads have been previously considered by some researchers. Detailed reviews of theoretical and experimental studies on pre-failure deformations of the circular plates can be found in published works: (Teeling-Smith and Nurick, 1991; Balden and Nurick, 2005; Shen and Jones, 1993; Lee and Wierzbicki, 2005a; Zajkani et al., 2010, 2012). To the best of current author's knowledge, a few works have been done on post failure behavior of the plates subjected to impulsive loads, so far. In those works, the main focus has been on empirical observations and finite element simulations; example is given in Lee and Wierzbicki (2005b).

\*Corresponding author. E-mail: [azajkani@gmail.com](mailto:azajkani@gmail.com), [azajkani@guilan.ac.ir](mailto:azajkani@guilan.ac.ir). Tel: +98131 6690275-9. Fax: +981316690271.

Menkes and Opat (1973) investigated dynamic behavior of beams under impulsive loading on the base of experimental observations and introduced three modes of failure which are the following:

1. First mode of failure, large inelastic deformation,
2. Second mode of failure, tensile tearing at the edges,
3. Third mode of failure, shear failure at the edges.

Teeling-Smith and Nurick (1991) carried out some experimental tests on explosive forming of the clamped circular plates, also. They observed that when the thickness of explosion materials increases, probability of the failure occurrence is proportionally raised. To predict second and third modes of the failure, Teeling-Smith and Nurick (1991) measured velocities of plates at clamped supports after full tearing. In addition, Nurick et al. (1996) presented various experimental results for the circular plates under explosive loadings. They considered initial stage of thinning as well as subsequent stages of the tearing on boundaries of plates. They used mild steel plates with 1.6 mm thickness and diameters of ranges 60 to 100 mm. They also used the following dimensionless parameter of impulse to illustrate dependence of the effective variables as follow

$$\phi = \frac{I}{\pi R h^2 \sqrt{\rho \sigma_y}} \quad (1)$$

where,  $I$ ,  $R$ ,  $h$ ,  $\rho$  and  $\sigma_y$  denote values of exposed impulse, radius of plate, thickness, density and yield stress of the material, respectively. In addition, they proposed the following intervals for each failure mode mentioned previously:

1.  $\phi \leq 47$ , First mode
2.  $47 \leq \phi \leq 95$ , Second mode
3.  $95 \leq \phi$ , Third mode

Applying flow rule at analytical investigations often creates some computational challenges for solution procedures. According to related references such as Jones (1997), concept of single moving hinge has been applied frequently in the upper bound- limit analyses of the rigid-perfectly plastic materials. It is worth mentioning that in some reports, neither the hinge idea and nor the flow rule have been used. In these cases, equation of energy balance (energy conservation) has been merely implemented, in order to simplify formulations of plasticity.

To predict deformation process of plate, Wen (1998) proposed an initial appropriate function. In order to obtain critical load which causes the second failure mode, he

presents a static solution considering work hardening effect. Zajkani et al. (2010) considered dynamic plastic responses of titanium, aluminum and steel plates subjected to large amplitude pulse loading. They adopted more complicated geometrical schemes representing deflection fields with the novel functions for the hinge motion. Applying the flow rule and strain rate effects, they produced a functional of energies and calculated unknown coefficients by the modified Ritz method. Gharababaei and Darvizeh (2010), Gharababaei et al. (2010), Gharababaei and Darvizeh (2011) and Babaei and Darvizeh (2012) obtained vertical mid-point deflection of the metallic plates (aluminum, copper and steel) subjected to impulsive loads. Methodologies of these works are: The modified Homotopy Perturbation method for solution of nonlinear equation (Gharababaei and Darvizeh, 2010), the singular value decomposition method (Gharababaei and Darvizeh, 2011), the balance of energy (Gharababaei et al., 2010; Babaei and Darvizeh, 2012) by using a zero-order Bessel function for deformation profile. Recently, Zajkani et al. (2012) have developed a pseudo-spectral collocation methodology to analyze high rate elasto-viscoplastic behaviors of the circular plates. By means of a relatively complex computational modeling, they solved incremental formulations of the differential equations and verified it by the finite element simulations. In that work, tearing of the plate was not considered, directly and an evolution of a porosity parameter is computed to evaluate effect of ductile material damage.

Jones (2010) reviewed some reports over the contributions of simple models, narrowly. He confirmed that those models can provide required facilities for designing constructions and assurance of the industrial plant against the high-intensity dynamic loading.

Using the motion equations, Jones and Alves (2010) studied the pre and post-failure behaviors of the beams and circular plates. In their dynamic solution, it is assumed that a moving plastic hinge is responsible for the deformation. According to this model, values of the critical loads for happening of the full severance or tearing of the plates are much lower than experimental amounts used in criteria at report (Teeling-Smith and Nurick, 1991). The main reason of this significant difference between analysis and experimental data is neglecting membrane stresses in the reference (Jones and Alves, 2010).

Although, present work like to other simple models does not cover overall aspects of the elastic-plastic deflections under high-rate loads but, it can present satisfactory accurate results. Herein, we remind capabilities of a simple model among this area in reference (Jones, 2012). The accuracies are normally achievable because, the principle parameters e.g. profile shape, strain rate and final time can be deduced from relevant experiments. So, these models are naturally capable of improving validations and assist designers to

consider preliminary judgment in risky cases. Nevertheless, despite a lot of existing data in this subject, there are significant differences on viewpoints, descriptions and quantities of the motion after failure occurrence of the plates.

Scaling amounts of the residual velocity plays a fundamental role to validate efficiency of a certain failure mechanism of the plate exposed by a pressure pulse. In our previous modelings (Zajkani et al., 2010, 2012; Gharababaei and Darvizeh, 2010, 2011; Gharababaei et al., 2010), we did not consider the tearing of plate and did not calculate the velocity of motion after local failure. Here, we will propose two new deformation models by effectively applying the yield line theory. Both models compute permanent deflection, straightforwardly and consider the deformation and motion after severance of the plate (post-local failure). The membrane forces and bending moments are considered, simultaneously. Two situations of deformation that is, pre and post-local failure are considered. Firstly, a new deformation model is considered by assuming the multi-stationary plastic hinges produced during deformation. These peripheral hinges are responsible for deformation and generate a spherical dome shape. Obtained results are compared with experimental data and some other works. In this state, a partial part of deformation that might be happened after severance is neglected. In the second model, final shape is considered by a conical shape, which is produced by a single peripheral moving hinge. In this part, comprising the transverse and radial motion of the plastic hinge, an alternate deformation procedure is proposed. Calculated plastic works of the deformation, energy absorbed in the boundaries at failure are obtained. In addition, calculating kinetic energy, the residual velocity of motion at outset of the local failure (second mode) is quantified more exactly as compared to existing models mentioned above. In order to verify obtained results, the ratios of the mid-point deflection respect to the thickness are illustrated, discussed and compared with the empirical data and other analyses.

## PRELIMINARY

Equilibrium equations of energy for the different failure modes can be easily written as follow:

1. First mode

$$E_{in} = E_{def} \quad (2a)$$

2. Second mode

$$E_{in} = E_{def} + E_{shear} + E_{residual} \quad (2b)$$

3. Third mode:

$$E_{in} = E_{shear} + E_{residual} \quad (2c)$$

where,  $E_{in}$ ,  $E_{def}$ ,  $E_{shear}$  and  $E_{residual}$  imply to input energy, deformation energy, shear energy and the residual energy, respectively.

Assuming that the energy dissipated through plastic work is equal to the input energy (initial kinetic energy) of the plate. According to the principle of momentum conservation, initial velocity induced by the impulsive load is:

$$V_0 = \frac{I}{m}, \quad m = \pi \rho R^2 h \quad (3)$$

$$E_{in} = \frac{1}{2} m V_0^2 = \frac{I^2}{2\pi \rho R^2 h} \quad (4)$$

As mentioned before, here a new mechanism is introduced and the present analysis established based on the mechanism and an approximate deformation function. Firstly, the function of transverse deflection is considered as a parabolic shape with power of  $b$

$$w = w_c \left( 1 - \left( \frac{r}{R} \right)^b \right) \quad (5)$$

In the dynamic loading analyses, in order to cover strain rate effects, dynamic yield stress  $\sigma_d$  is used instead of static yield stress  $\sigma_y$  by  $\sigma_d = \lambda \sigma_y$ . Here, coefficient of  $\lambda$  can be obtained by an empirical material model such as the Cowper-Symonds constitutive equation (Jones, 1997). In this model, dynamic yield stress will be a function of the strain rate and material parameters as follow:

$$\lambda = \left( 1 + \left( \frac{\dot{\epsilon}^p}{\dot{\epsilon}_c} \right)^q \right) \quad (6)$$

where  $\dot{\epsilon}^p$  is average of the plastic strain rate, and  $\dot{\epsilon}_c$  and  $q$  are the material constants. The value of  $\dot{\epsilon}^p$  can be estimated for moderate deflection of the plate. In addition, radial strain indicates main portion of the strain distributions of deformation and its rate can be used to evaluate  $\dot{\epsilon}^p$ . Moreover, strain calculation approximates maximum value of the radial strain equal to 0.19 and 0.089 for the uniform and localized distributions of loading, respectively. In addition, Bodner and Symonds (1979) and Nurick (1985) reported that deflection of the blast loaded plates reach their maximum amounts

approximately at  $120 \mu s$ . So, it implies that for the parabolic prediction shape of deflection, values of the average strain rate for the uniform distribution of loading will be about  $1583 s^{-1}$  and  $3750 s^{-1}$  for  $b = 2$  and  $3$ , respectively. Also for the localized distribution of loading, it shows  $\dot{\epsilon}^p$  equal to  $742 s^{-1}$ . Therefore, average of  $\lambda$  can be obtained if the mentioned value for  $\dot{\epsilon}^p$  and material constants  $\dot{\epsilon}_0$  and  $q$  are considered in Equation (6). In order to simplify Equation (6) and make conversion of the solution,  $\lambda$  will be considered constantly as the same of references (Gharababaei and Darvizeh, 2010, 2011; Gharababaei et al., 2010). It is remarkable to mention that if an appropriate  $\lambda$  is estimated for threshold stage of the failure, despite of being constant value; we can expect satisfactory results in this short time deformation.

**LOCAL FAILURE (PERIPHERAL RUPTURE OR TEARING) CRITERION**

Firstly, it is assumed that failure is occurred at the support region and it is taken apart from clamped edge. Consequently, a full severance of the plate will be occurred after a specific sliding from support. The amount of sliding can be written as follow (Gupta and Nagesh, 2007):

$$\Delta^s = \gamma e \tag{7}$$

where,  $\gamma$  is the shear strain and  $e$  is half length of the plastic hinge at the supports. The critical sliding, where the complete severance can be happened, is:

$$\Delta_{cr}^s = \gamma_{cr} e \tag{8}$$

where,  $\gamma_{cr}$  is the critical shear strain obtained experimentally. It is 0.8 for mild steel and 0.5 for aluminum alloy (Yu and Chen, 2000). Shen and Jones (1993) proposed an approximate equation regarding the length of the plastic hinge  $L_h$  with dissipated energy ratio,  $\beta$ . To find  $L_h$ , the following equation can be utilized

$$\alpha + 1.2\beta = 1.3 \tag{9a}$$

$$\alpha = \frac{L_h}{h} = \frac{2e}{h} \tag{9b}$$

$$\beta = \frac{E_{shear}}{E_h} \tag{9c}$$

where,  $E_{shear}$  and  $E_h$  are the shear force energy and the plastic work in the circular plastic hinge formed at the support, respectively.

For occurrence of the second failure mode, which is desirable here, Shen and Jones (1993) proposed parameter of  $\beta \leq 0.45$ . Using Equation (9), we can obtain:  $e \geq 0.38 h$ . According to available critical amounts of  $\gamma_{cr}$ , the minimum amount of  $\Delta_{cr}^s$  can be obtained about  $0.304 h$  for the steel and  $0.19 h$  for the aluminum 1200 H4 alloys. These values are quite similar to the experimental data reported in Jouri and Jones (1988). It can be supposed that deflection quantity is equivalent with a coefficient of thickness;  $k h$ . Therefore, this point is mentioned that a complete severance will happen at a definite critical coefficient of thickness as  $k_{cr}$ , which can be evaluated. Here, the least amount of this quantity is obtained as  $0.304$  and  $0.19$  for the steel and aluminum, respectively. Similarly, its highest amount is obtained about 0.4 and 0.25 for the steel and aluminum, respectively. Here, we assume that the critical sliding is changed linearly with respect to input impulse. So, on the basis of the second failure mode, the critical sliding for the mild steel and aluminum alloys can be written as:

$$k = \begin{cases} 0.25 + \frac{0.06(47 - \phi)}{48} & \text{Aluminum 1200 H4} \\ 0.4 + \frac{0.096(47 - \phi)}{48} & \text{Mild steel} \end{cases} \tag{10}$$

**DEFORMATION SCHEME-MULTI HINGES MODEL**

Basically, the limit analysis are derived from virtual work and categorized by the approximate theories. Practically, concept of the flow rule is closer to nature of the plastic deformation; more exact than the limit analysis. Since applying a limit analysis simplifies problems, here adopting a multi hinges model would be much beneficial. This task is the same of plastic node method expressed in Ueda and Yao (1982). In many cases of the finite element analysis of plasticity, the flow rule can be stated as a procedure that plastic deformation is considered at the plastic hinges. This attitude to the elastic-plastic problems can facilitate applying concept of the flow rule in the continuum mechanics. In the finite element modeling of metal forming process, implementing the flow rule through the nodal yielded lines reduces computational efforts, drastically (Kobayashi et al., 1989). Herein, concept of the multi hinge is that the yield function is checked only at each peripheral node in domain of interest and stress resultants satisfy the yield

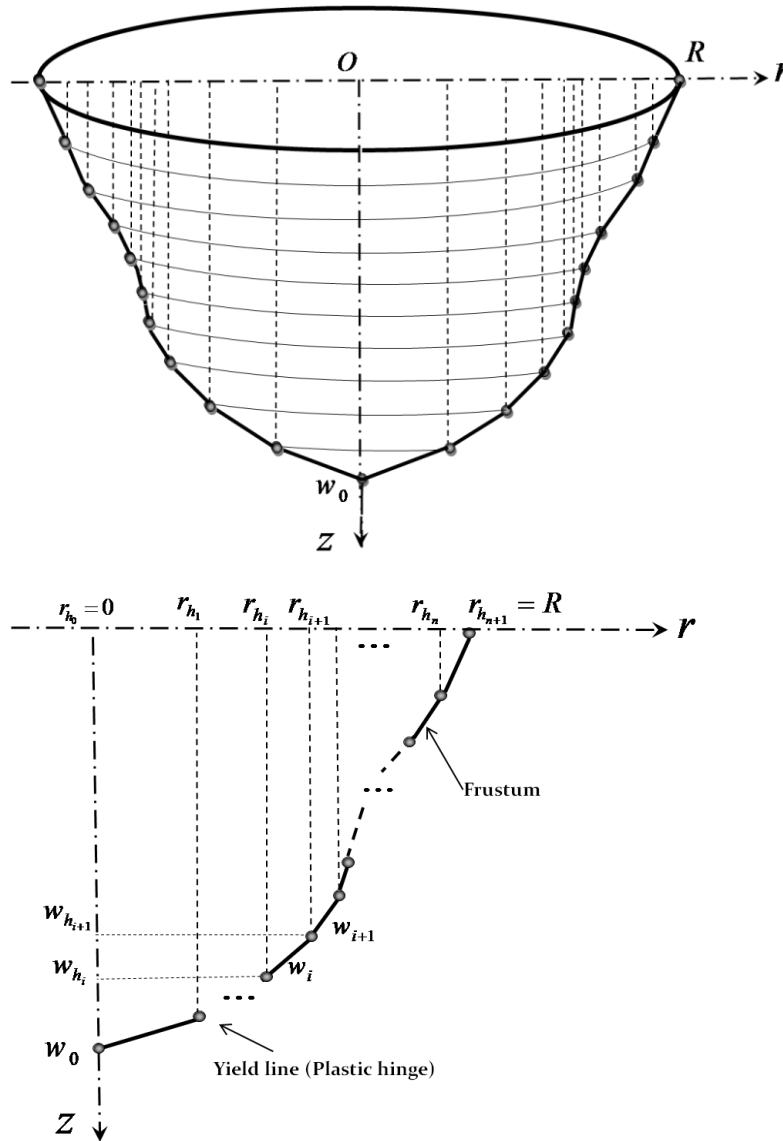


Figure 1. Dome shape deformation scheme modeled by multi plastic hinges.

condition while the interior of an annular element remains elastic. Figure 1 illustrates deformation scheme for the multi hinges model.

According to this model, loading process produces several circular yield lines (plastic hinges) during deformation of plate. In this case, the distances between the plastic hinges are supposed by several frustums. In the conical areas, radial curvatures will be zero. So, the works done by the radial bending moments are zero, while these moments at the plastic hinges are on the yielded limit. Generally, at the high -rate amplitude of the pressure pulse, the plate moves closer to the rigid-perfectly plastic scheme. At first glance, if the internal parts are supposed by elastic elements, it leads to include vibrating effect and spring backs in deflection. Alternately, at the high velocity forming of the plate, the

snap and spring backs can be ignored. So, it is concluded that each frustum between two subsequent hinges can behaves plastically. Moreover, three types of the hinges distribution are examined. At first, the distances between the subsequent hinges are taken constant. Considering  $n$  plastic hinge, radial positions of the hinges would be as follow

$$r_{h_{i-1}} = \frac{(i-1)R}{n+1}; \quad i = 1, \dots, n+1 \tag{11}$$

where the central hinge is at  $r_{h_0} = 0$  and the last hinge prior the support is accounted by  $r_{h_n}$ . The vertical

displacement of the hinges can be written in the following form ( $b = 2$ )

$$w_{h_i} = w_0 \left( 1 - \left( \frac{r_{h_i}}{R} \right)^2 \right) \tag{12}$$

It is assumed that the circumferential bending moment throughout the plate reaches the yield point. The deflection function of plate between hinges is:

$$w_i = -w_{h_{i-1}} + \left( \frac{w_{h_i} - w_{h_{i-1}}}{r_{h_i} - r_{h_{i-1}}} \right) (r - r_{h_{i-1}}) \tag{13}$$

According to the relation (13), the radial and circumferential membrane strains between subsequent hinges would be as follow:

$$\epsilon_r = \frac{1}{2} \left( \frac{\partial w_i}{\partial r} \right)^2 + z k_r \tag{14a}$$

$$\epsilon_\theta = z k_\theta \tag{14b}$$

Also, the values of curvatures can be obtained

$$k_r = -\frac{\partial^2 w_i}{\partial r^2} = 0 \tag{15a}$$

$$k_\theta = -\frac{1}{r} \frac{\partial w_i}{\partial r} = \frac{1}{r} \frac{w_{h_{i-1}} - w_{h_i}}{r_{h_i} - r_{h_{i-1}}} = \frac{w_0(2i-1)}{(n+1)Rr} \tag{15b}$$

So, Equations (15) result

$$\epsilon_r = \frac{1}{2} \frac{w_0^2(2i-1)^2}{(n+1)^2 R^2}, \tag{16a}$$

$$\epsilon_\theta = \frac{z w_0(2i-1)}{(n+1)Rr} \tag{16b}$$

### CALCULATING THE PLASTIC WORKS

The total plastic work  $E_p$  includes energies of the deformation  $E_{d\&f}$  and shearing failure  $E_{sh\&ar}$  as follow:

$$E_p = E_{sh\&ar} + E_{d\&f} \tag{17}$$

$E_{d\&f}$  is defined by the plastic works of the radial and circumferential membrane forces ( $E_{N_r}$  and  $E_{N_\theta}$ ), the radial and circumferential bending moments ( $E_{M_r}$  and  $E_{M_\theta}$ ), and the plastic works dissipated by internal hinges ( $E_h$ ) and the hinge on edge support ( $E_{M_s}$ ) as follow:

$$E_{d\&f} = E_{N_r} + E_{N_\theta} + E_{M_r} + E_{M_\theta} + E_h + E_{M_s} \tag{18}$$

### WORKS OF MEMBRANE FORCES

Using the Tresca yield condition criteria and flow rule with rigid –perfectly plastic material, it could be assumed that  $\sigma_r = \sigma_d$ . Using Equation (16a), work of radial force in each cone would be obtained as follow:

$$E_{N_r} = \int_{r_{h_{i-1}}}^{r_{h_i}} \int_{-\frac{h}{2}}^{\frac{h}{2}} 2\pi r \sigma_d \epsilon_r dz dr = \frac{\pi \sigma_d h w_0^2 (2i-1)^3}{2(n+1)^4} \tag{19}$$

So, work of all elements are added to give

$$E_{N_r} = \frac{\pi \sigma_d h w_0^2}{2} \sum_{i=1}^{n-1} \frac{(2i-1)^3}{(n+1)^4} = \frac{\pi \sigma_d h w_0^2 (2n^4 + 8n^3 + 11n^2 + 6n + 1)}{2(n+1)^4} \tag{19b}$$

Similarly, plastic work of the circumferential force throughout plate domain is evaluated for as

$$E_{N_\theta} = \sum_{i=1}^{n+1} \int_{r_{h_{i-1}}}^{r_{h_i}} \int_{-\frac{h}{2}}^{\frac{h}{2}} 2\pi r \sigma_d \epsilon_\theta dz dr = 0 \tag{20}$$

### WORK OF BENDING MOMENTS

The work of radial and circumferential bending moments can be calculated as

$$E_{M_r} = 0 \tag{21a}$$

$$E_{M_\theta} = \sum_{i=1}^{n+1} \int_{r_{h_{i-1}}}^{r_{h_i}} 2\pi r M_d k_\theta dr \tag{21b}$$

where  $M_d = \sigma_d h^2 / 4$ .

Substituting (12) to (15) into Equation (21b) leads to simplify it as follow:

$$E_{M_6} = \sum_{i=1}^{n-1} \frac{\pi \sigma_d h^2 w_0 (2i-1)}{2(n+1)^2} = \frac{\pi \sigma_d h^2 w_0}{2} \quad (22)$$

## PLASTIC SHEARING FAILURE WORK AT THE SUPPORT

Plastic work of the shearing force at support can be calculated as

$$E_{shear} = 2\pi R Q_d k h$$

$$Q_d = \sigma_d h$$

where  $Q_d$  is shear stress when it reaches the dynamic yield stress.

## WORK OF PLASTIC HINGES

Considering the deformation profile, plate slope at the support is as follow:

$$\varphi_s = \frac{-w_0(2n+1)}{R(n+1)} \quad (24)$$

So, the work done by this force component is

$$E_{M_5} = -2\pi R \varphi_s M_d = \frac{w_0 \pi \sigma_d h^2 (2n+1)}{2(n+1)} \quad (25)$$

On the other hand, works of other internal hinges can be calculated, easily. Rotation angle of the  $i^{\text{th}}$  hinge can be expressed as a function of the radial and vertical position of neighbor hinges

$$\varphi_i = \frac{w_{r_{i+1}} - w_{r_i}}{r_{i+1} - r_i} - \frac{w_{r_i} - w_{r_{i-1}}}{r_i - r_{i-1}} = \frac{2w_0}{(n+1)R}; \quad i = 1, \dots, n \quad (26)$$

Considering above equation, the work of the internal hinges is obtained

$$E_h = \sum_{i=1}^{n-1} 2\pi r_{h_i} M_d \varphi_i = \frac{\pi \sigma_d h^2 w_0 (n+2)}{2(n+1)} \quad (27)$$

Consequently, according to relations (17) to (27), we have

$$E_{def} = \frac{\pi \lambda \sigma_y h w_0}{2} \left( \frac{w_0 (2n^2 + 8n^3 + 11n^2 + 6n + 1)}{(n+1)^2} + 4h \right) \quad (28)$$

and

$$E_p = 2\pi R \lambda \sigma_y h^2 + \frac{\pi \lambda \sigma_y h w_0}{2} \left( \frac{w_0 (2n^2 + 8n^3 + 11n^2 + 6n + 1)}{(n+1)^2} + 4h \right) \quad (29)$$

By equating relation (29) with input energy (4) and using dimensionless impulse (1), the mid-point deflection of plate can be obtained

$$\frac{w_0}{h} = \sqrt{\frac{4(n+1)^2}{(2n^2 + 8n^3 + 11n^2 + 6n + 1)} \left( \frac{(n+1)^2}{(2n^2 + 8n^3 + 11n^2 + 6n + 1)} + \frac{\phi^2}{4\lambda} - k\mu \right)} \quad (31)$$

where  $\mu = R/h$ . When pressure pulse is less than the critical value,  $k$  is taken zero. In the final limit state ( $n \rightarrow \infty$ ) that the hinges have too small distances from together, Eq. (30) will be evaluated as

$$\frac{w_0}{h} = \sqrt{1 + \frac{\phi^2}{2\lambda} - 2\mu k - 1} \quad (31)$$

## EFFECT OF HINGES NUMBER

To investigate the effect of hinges number on the computed results, several numbers are examined by comparisons between calculated plastic works and the equation proposed in reference (Teeling-Smith and Nurick, 1991). In this reference, some experiments on the circular steel plate with thickness of **1.6 mm** have been carried out and the following equation for deformation energy has been proposed for the second failure mode

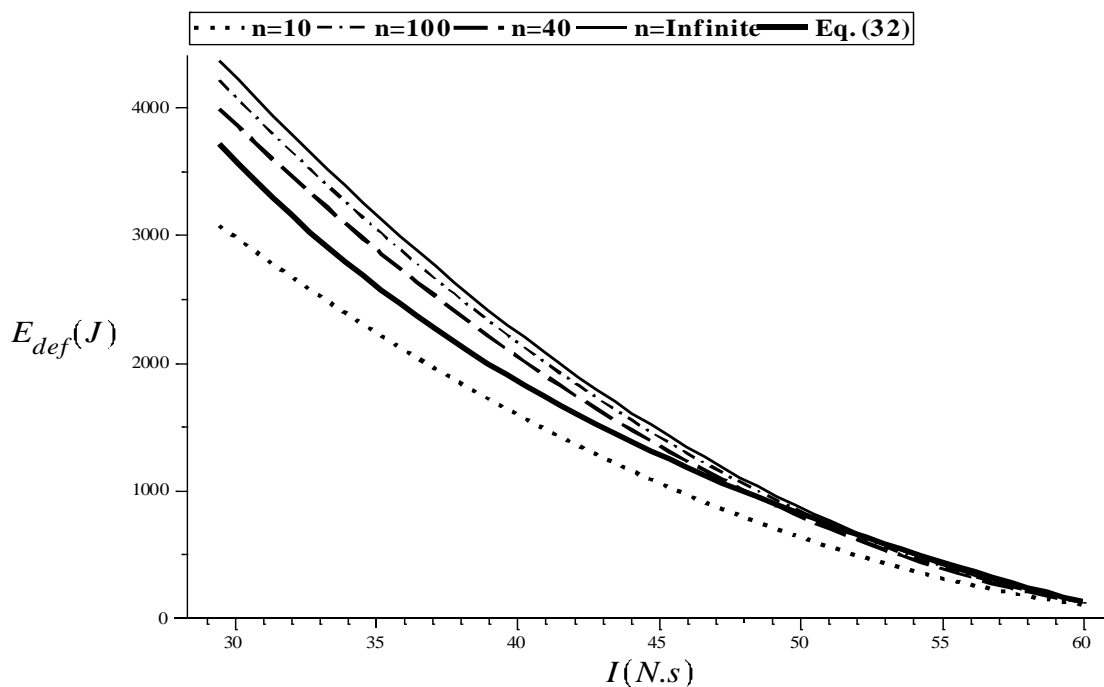
$$E_{def} = \frac{328835.34}{\phi} - 3350 \quad (32)$$

The material properties present in the Table 1 are used to show the results.

Considering the relevant relations, it can be expected that less plastic work is necessary for lower number of hinges. In Figure 2, amounts of plastic works at the second failure mode have been illustrated per different number of hinges. For these calculations, material is mild steel and radius of plate is 50 mm. The result with  **$n = 20$**  has a good compatibility with the relation proposed by (Teeling-Smith and Nurick, 1991). It is also observed that by increasing the hinges number, the

**Table 1.** Properties of the plates used in the analysis (radiuses of the plates are 50 mm).

Material	Thickness $h(mm)$	Yield stress $\sigma_y(MPa)$	$\rho(Kg/m^3)$	$\lambda$
Mild steel	1.6, 2 and 3	318	7800	3.08
Copper	2 3	277 201	8940	2.65
Aluminum 1200 H4	2 and 3	120	2700	1.87

**Figure 2.** The plastic work versus input impulse for mild steel (1.6 mm).

deformation plastic work grows. In the Figure 3, ratios of the residual velocity at the second failure mode respect to initial velocity are shown per different hinges number.

Using Equation (29) it is possible to obtain the mid-point deflection of the plate versus imparted impulses. Some experimental results have been presented in Gharababaei and Darvizeh (2011). In Table 2, some proposed relations for dimensionless mid-point deflection/thickness of a circular plate under uniform distribution of impulsive loading have been summarized.

In Figures 4 to 6, results are compared with the experiments done by (Gharababaei et al, 2010) and two theoretical models proposed by (Symonds and Wierzbicki, 1979) and (Nurick and Martin, 1989). These models are corresponds with two first equations of Table 2. In Figure 4 to 6, the mild steel plate with thickness of 1.6 mm, the aluminum plate with thickness of 2 mm and the copper plate with thickness of 2 mm have been used,

respectively.

As seen in figures, whenever the number of hinges increases, results of the modeling follow the experimental data more closely.

## THE EFFECT OF NON-UNIFORM HINGES DISTRIBUTION

Previously, it was assumed that the hinges distributions are located uniformly at the radial distance of the plate. Here, two different schemes are proposed for the non-uniform distribution of the hinges. Similarly, new obtained results are compared with the experimental and theoretical data. At the first case of non-uniform distribution of hinges (C1), a hinge distribution is considered by a condition that distances between adjacent hinges at the center areas are closer together



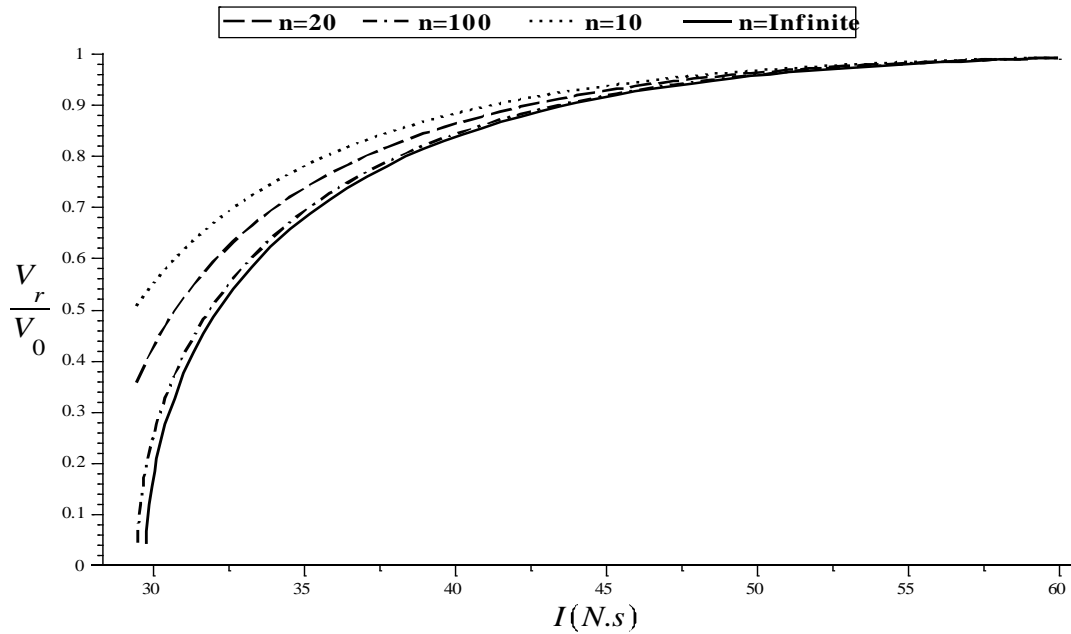


Figure 3. The ratio of residual velocity to initial velocity.

Table 2. Proposed relations for mid-point deflection thickness ratio for circular plate under explosive loads (Nurick and Martin, 1989).

Researchers	Relations
Symonds and Wierzbicky	$\frac{w_0}{h} = 0.665\phi$ (33a)
Nurick and Martin - (model I)	$\frac{w_0}{h} = 0.424\phi$ (33b)
Hudson	$\frac{w_0}{h} = 0.998\phi$ (33c)
Lipman	$\frac{w_0}{h} = 0.415\phi$ (33d)
Jones	$\frac{w_0}{h} = 0.817\phi$ (33e)
Batra and Dubey	$\frac{w_0}{h} = 1.200\phi$ (33f)

rather than other areas near the boundaries. In this case, the function of hinges distribution is supposed to be as follow

$$r_{hi} = \frac{i^2 R}{(n + 1)^2} \tag{34}$$

The plastic deformation work could be obtained in a similar way mentioned before. At the limit state, in which number of the hinges are infinite, results are obtained as the same of previous part, but for the limited number of

the hinges, different results are seen. In Figures 7 to 10, results of the residual velocities and plastic deformation works are compared with the case of the uniform distribution of hinges.

To evaluate the effect of case C1, amounts of the plastic deformation works are compared with the uniform hinges distribution in the Figure 8.

According to illustration, plastic work of case C1 is lower than the uniform distribution at the same number of hinges. But by increasing the number of hinges, the plastic deformation works are getting convergent together. Figure 9 displays the residual velocity-initial

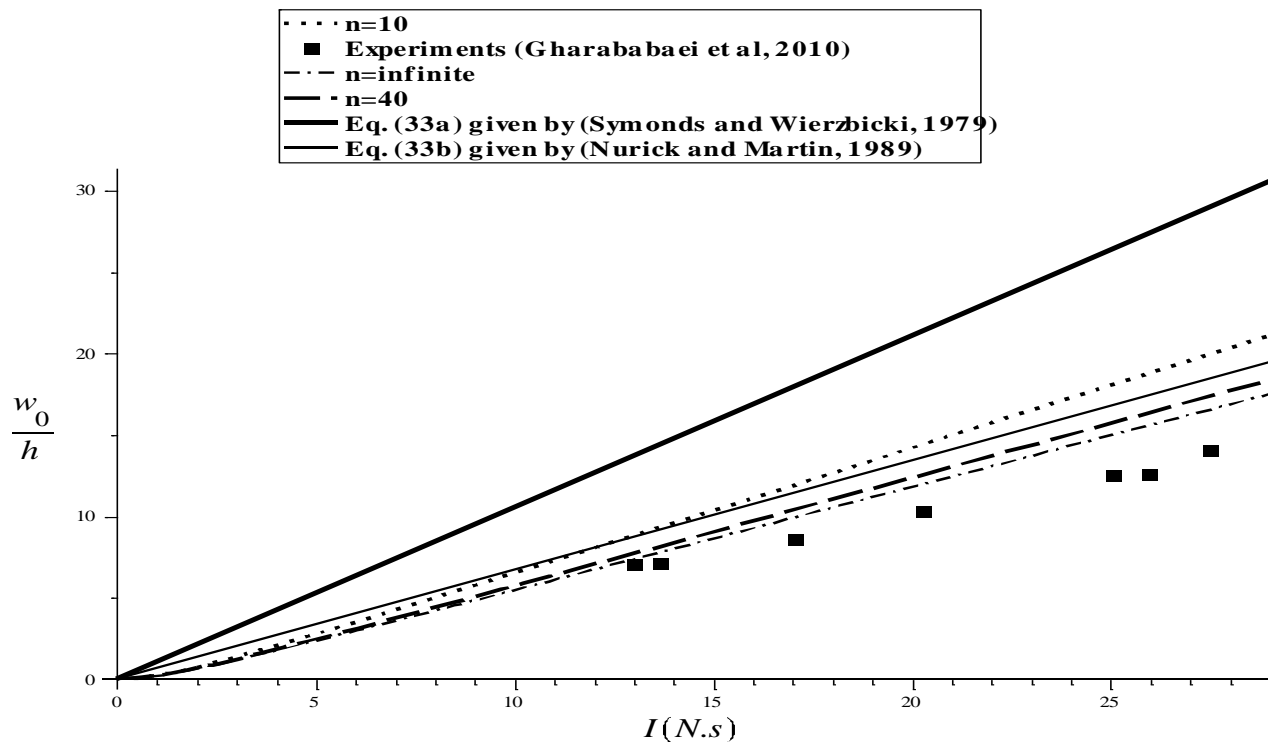


Figure 4. The mid-point deflection thickness ratios versus impulse for mild steel plate (1.6 mm thickness).

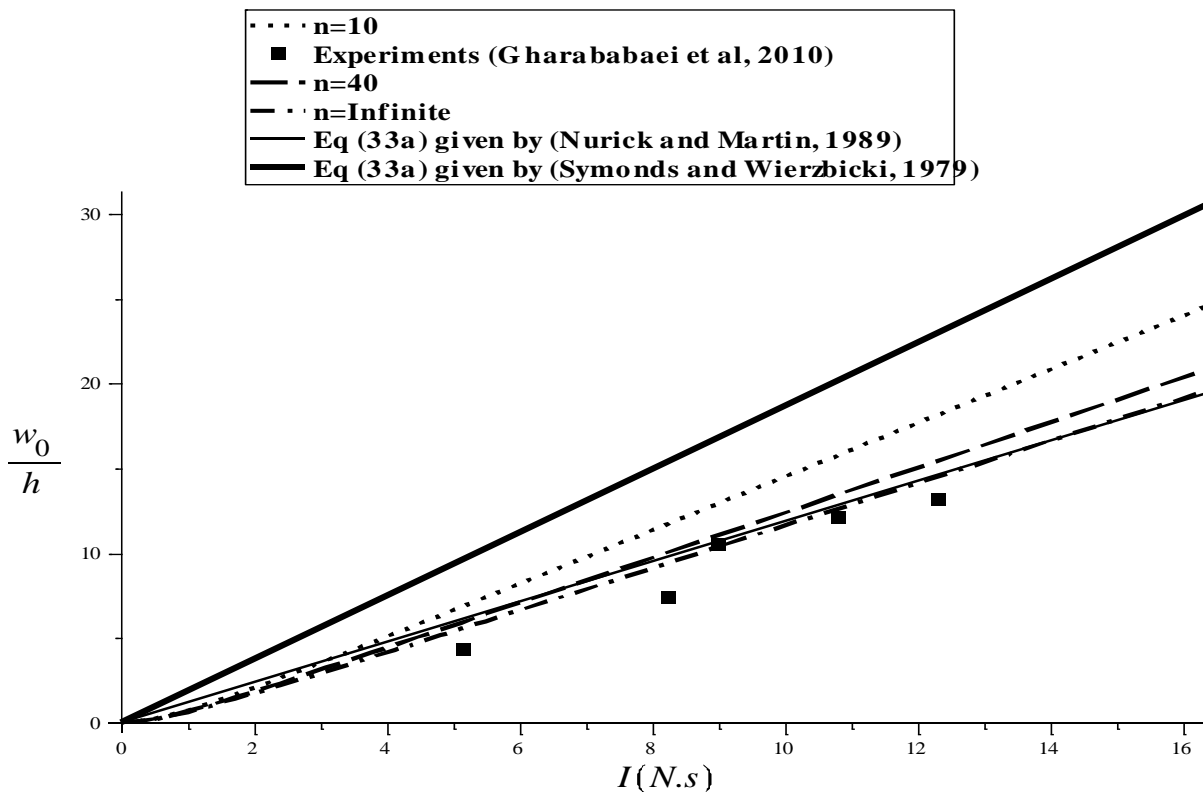


Figure 5. The mid-point deflection thickness ratios versus impulse for aluminum plate (2 mm thickness).

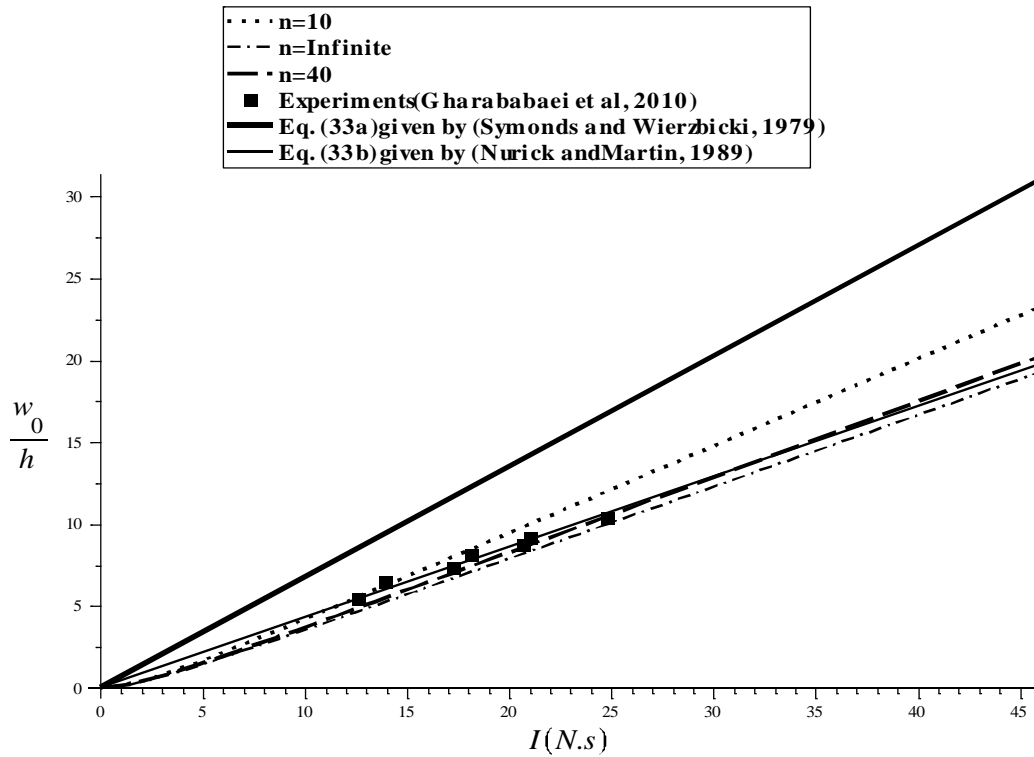


Figure 6. The mid-point deflection thickness ratios versus impulse for copper plate (2 mm thickness).

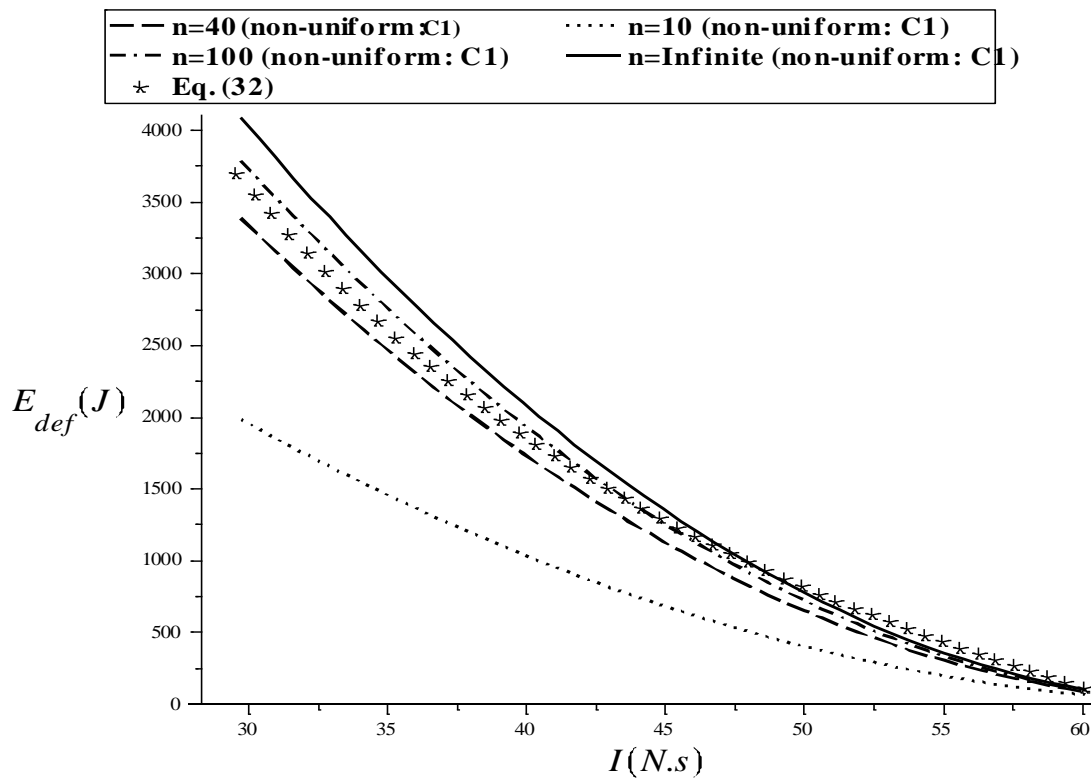
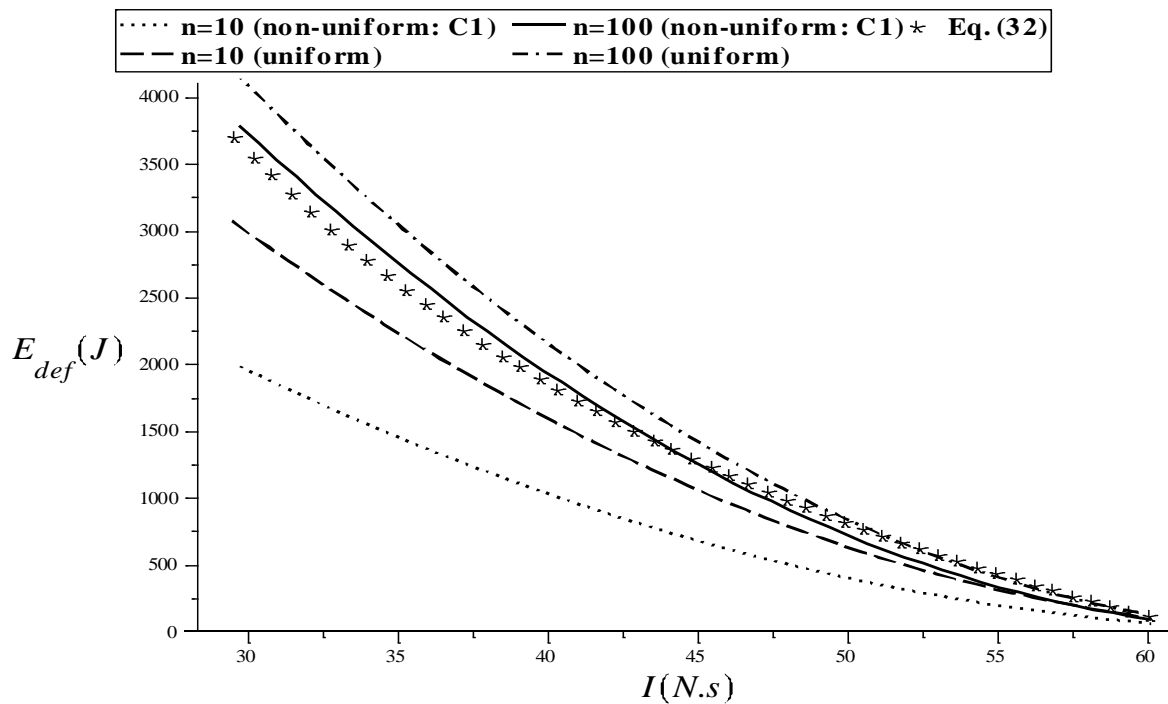
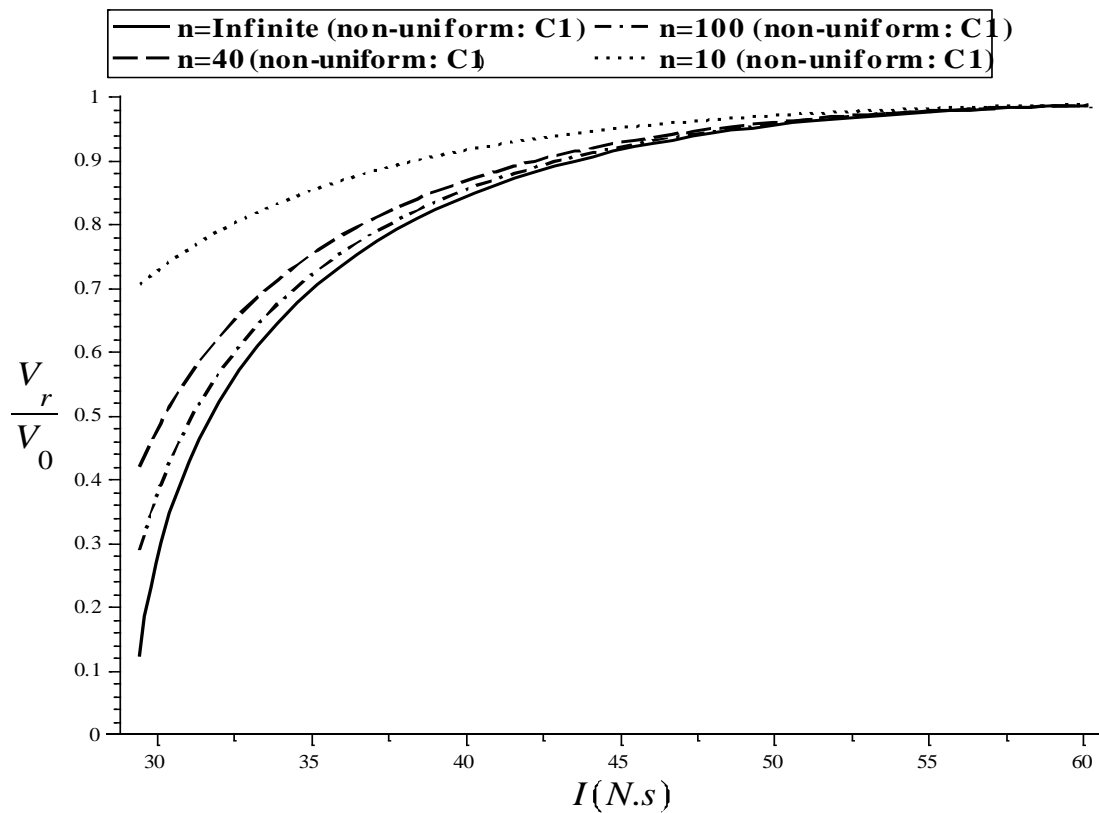


Figure 7. The deformation plastic works versus impulses for mild steel plate (1.6mm); first case of non-uniform hinge distribution (C1).



**Figure 8.** The deformation plastic works for mild steel (1.6 mm); comparisons between case of C1 non-uniform hinge distribution and uniform distribution.



**Figure 9.** The residual velocity initial velocity ratio versus input impulse for mild steel (1.6mm); first case of non-uniform hinges distribution (C1).

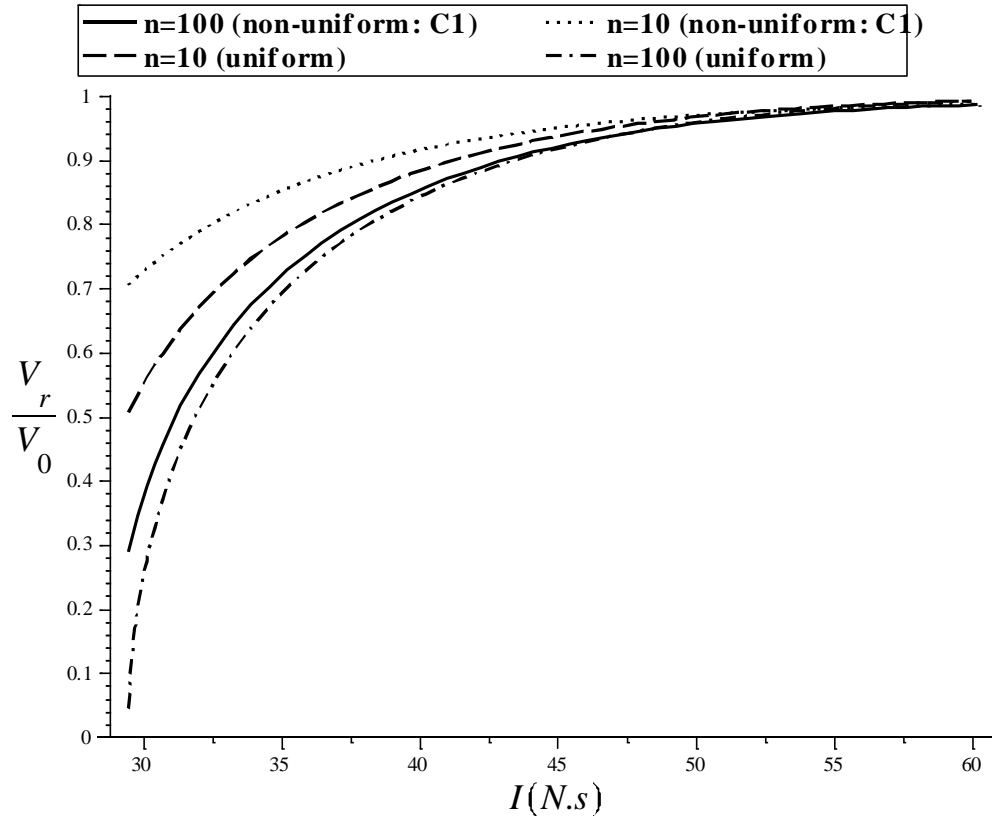


**Figure 10.** The ratios of residual velocity to initial velocity for mild steel (1.6 mm); comparisons between case of C1 non-uniform and uniform hinges distribution.

velocity ratio versus imparted impulses.

To be better comparison of the effect of hinge numbers, results have been plotted in Figure 10 for the numbers of 10 and 100 hinges.

In the previous case for C1, the effect of hinges distribution scheme was investigated for the circumstance that hinges aggregation at center area is more than boundary. In the second case of non-uniform hinges distributions (C2), which it is reverse of C1, the aggregation of hinges at areas near center is less than the boundary. Therefore, this distribution function of hinges would be as follow

$$r_{hi} = \frac{\sqrt{i} R}{\sqrt{n+1}} \tag{35}$$

Figure 11 shows the plastic deformation energies versus imparted impulses at case C2.

For better comparison between two schemes of the non-uniform hinges distributions, deformation energies of patterns C1 and C2 are plotted in the Figure 12. In pattern C2, the results are converging faster than C1. At the large numbers of hinges, two patterns are

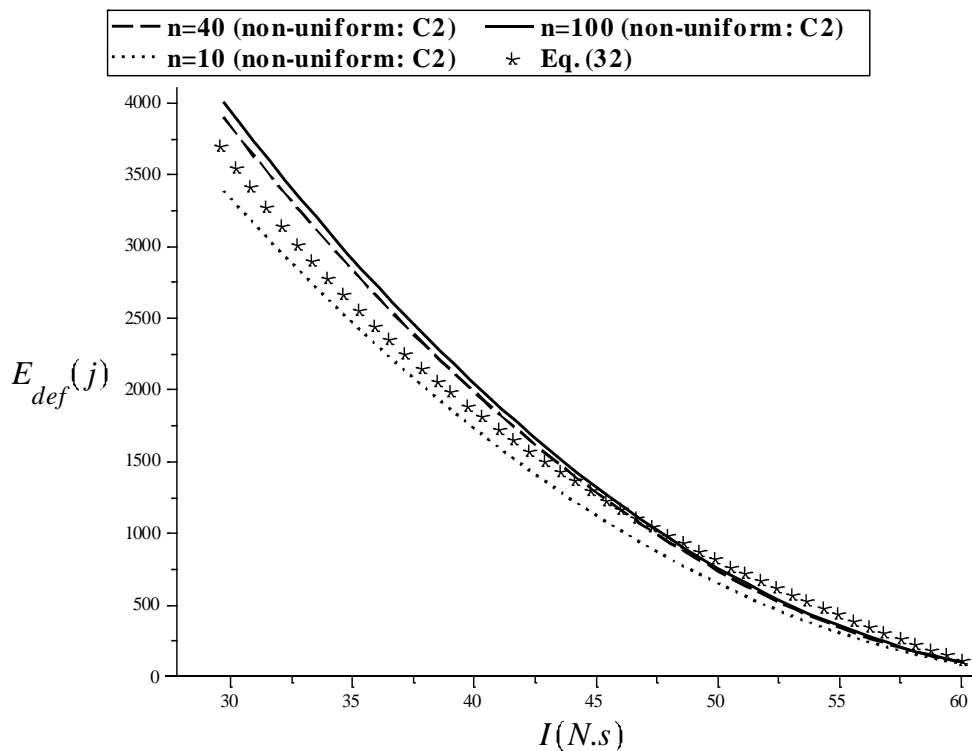
approximately compatible together. Here, it can be found that the pattern C2 could be more reasonable, lower volume of calculations and better responses.

As mentioned previously, there is no enough attention to consider behavior of the plate exactly when it takes apart from its support. Here, using the criteria stated in present study, a total energy required for deformation severance of plate can be obtained. Considering amount of input energy of imparted impulse, the residual energy after severance will be acquirable. Herein, it should be noted that the deformation after severance is neglected.

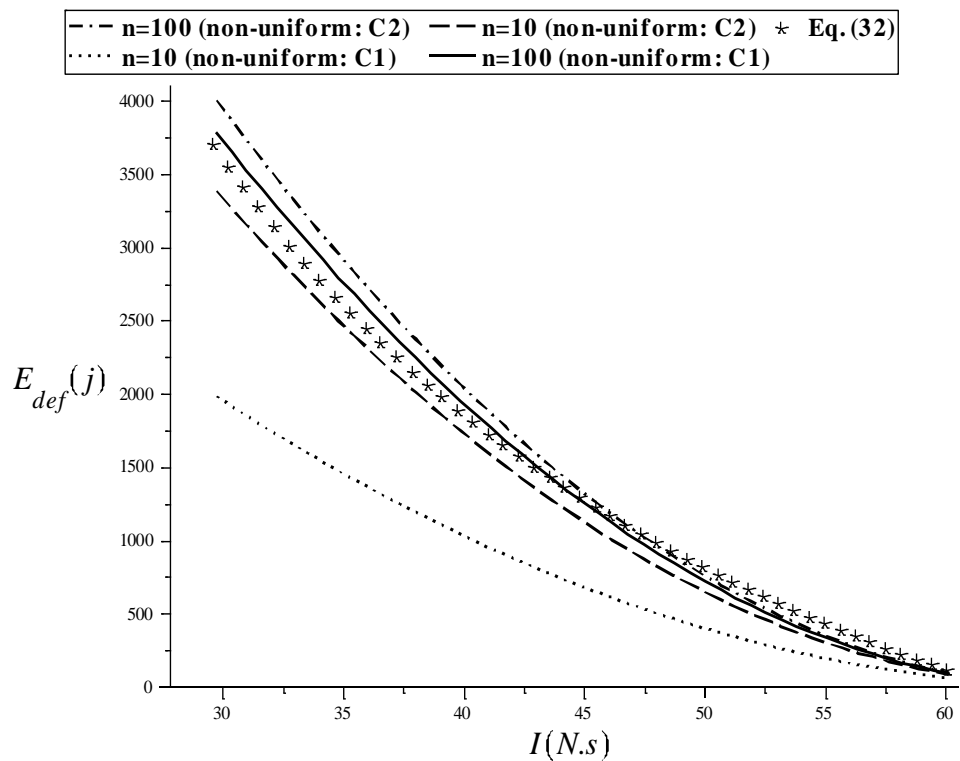
In Figure 13, the effect of hinges distribution pattern are compared again by the ratios of residual velocity respect to initial velocity per 10 and 100 hinges.

Table 3 presents the root mean square errors (RMSE) for three metallic materials and different numbers of the hinges. The experimental data have been chosen from reports in Gharababaei and Darvizeh (2010) and Gharababaei et al. (2010). Generally, these comparisons indicate that increasing the number of hinges causes more compatibility of results with the experimental data else copper plate.

A lot of examples can be found in Gharababaei et al. (2010) to compare more specimens. Table 4 indicates



**Figure 11.** The deformation plastic works versus impulses for mild steel plate (1.6 mm); second pattern of non-uniform hinges distribution (C2).



**Figure 12.** The deformation plastic works versus impulses for mild steel plate (1.6 mm); comparison between patterns of C1 and C2 as two non-uniform hinges distributions.

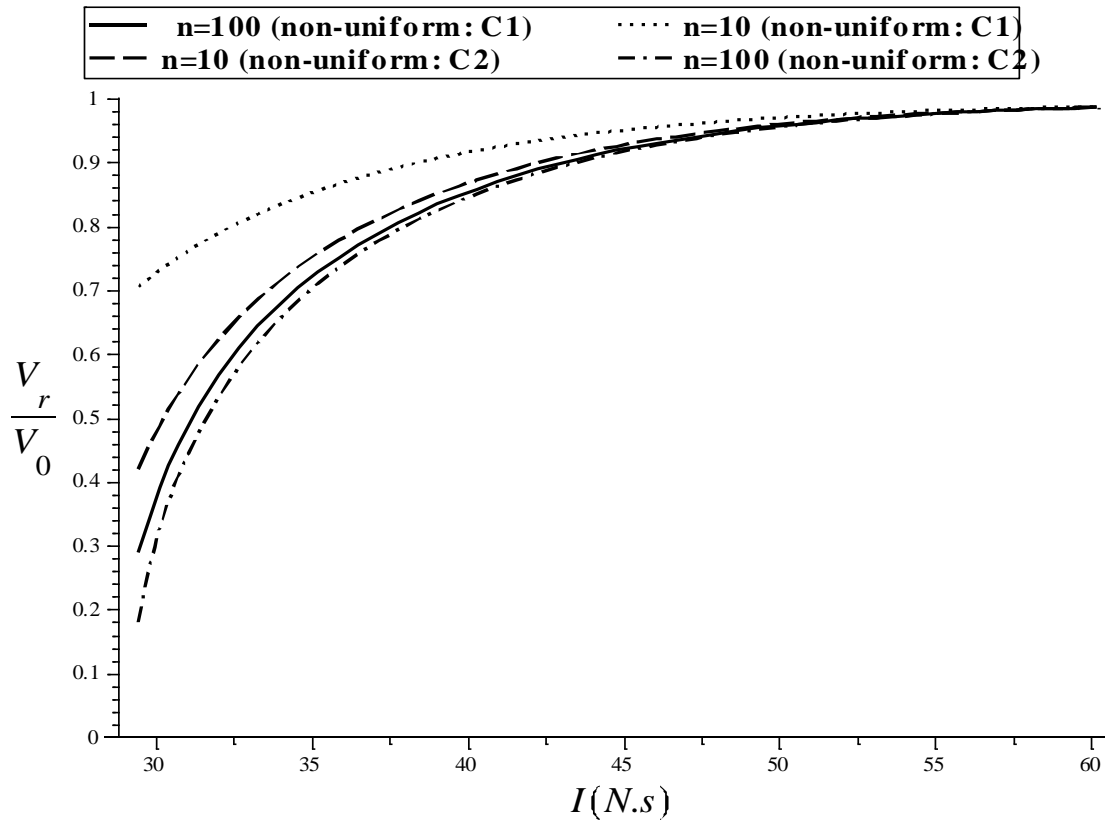


**Figure 13.** The ratio of residual velocity initial velocity versus impulses for mild steel plate (1.6 mm); comparison between patterns of C1 and C2 as two non- uniform hinges distributions.

**Table 3.** The root mean square errors (RMSE) for different numbers of the hinges.

Material	Thickness $h(mm)$	RSME			
		$n = 10$	$n = 40$	$n = 100$	$n \rightarrow \infty$
Mild steel	1.6	4.32	2.49	2.14	1.9
	2	2.43	1.33	1.12	0.99
Copper	2	0.73	0.61	0.75	0.87
	3	0.46	0.9	0.99	1.06
Aluminum 1200 H4	2	3.66	2	1.7	1.51
	3	1.54	0.58	0.4	0.28

calculations of the root mean square errors for the mid-point deflection ratios by other models. As it is seen, this study often introduces better predictions in comparison with the others works.

**DEFORMATION SCHEME - CONICAL MODEL**

The final shape of deformation is a function of the many

parameters. Here, a condition is considered that the final deformation shape is a conical shape. Among the various loading conditions, if the stand-off distance is less than the radius of plate, this condition is normally named by the localized loading. In this case, the final shape is almost a conical form. However, in practical situations, the final shape is not a complete cone. So, an idealized situation will be considered here, which the final deformation is a complete cone. Therefore, computed

**Table 4.** The root mean square errors (RMSE) of various models for experimental data (Gharababaei et al., 2010).

Researchers	RMSE
Symonds and Wierzbicky	7.208
Nurick and Martin - (model I)	2.017
Hudson	14.53
Lipman	1.833
Jones	10.523
Batra and Dubey	18.977

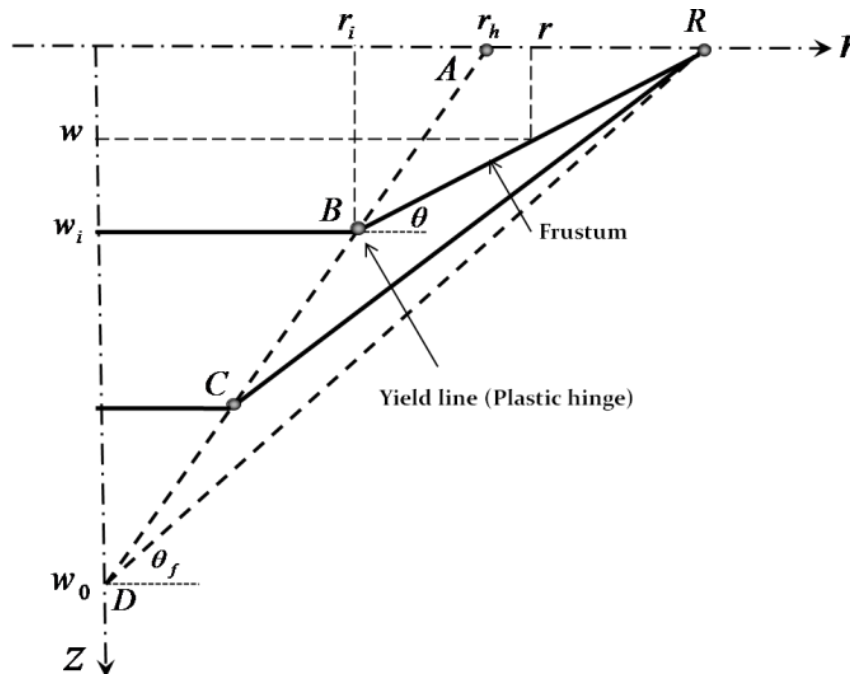


**Figure 14.** The conical deformation scheme modeled by a single plastic hinge. where,  $R$  is radius of plate,  $w_0$  is the final mid-point deflection and  $\theta_f$  is the final angle with respect to the horizon.

results are compared with the relevant experimental data, which the final deformation is not exactly a cone but, it has a little radial curvature. Here, an alternate deformation mechanism is proposed by using a new motion of a single circular plastic. The conical deformation mechanism is shown in Figure 14.

Actually, deformation is complemented by the radial and vertical motion of the hinges. The end of deformation is the instance that the hinge reaches the center of plate. Here, using an energy approach, the mid-point deflection of the plate is evaluated, straightforwardly. Also, the threshold energy and impulse, which are necessary for the complete tearing of plate, are obtained, analytically. Firstly, a shear sliding at the boundary is considered by the factor of tearing. Assuming that upon mechanism

reaches the first stage of critical sliding; complete tearing will be taken place. The redundant energy, which is more than the required value of the complete tearing mid deformation, is converted to the kinetic energy. The other part of the deformation that might be happened after the tearing is neglected.

Point of  $A$  at distance of  $r_h$  from the center is the initial position of the hinge. It is assumed that the plastic hinge moves over a straight line  $DA$  to get to the final position. As mentioned before, the deformation is performed as a process through motions of the radial and vertical plastic hinges. This procedure is completed so that the circular hinge becomes small until it reaches the center. In this moment, it is assumed that the sliding at the support causes the complete tearing and the deformation



mechanism. If there is more energy than is needed for the deformation and tearing, it converts to kinetic energy of the plate after severance. Point B in Figure 14, represents the condition of the hinge when it is at distance  $r_i$  from the center with the vertical displacement  $w_i$ . So, the cone will have an angle of  $\theta$  with respect to the horizon as follow:

$$\theta = \frac{w_i}{R - r_i} \quad (36)$$

Thus, the final angle would be:

$$\theta_f = \frac{w_0}{R} \quad (37)$$

Also,  $w_i$  could be obtained as follow:

$$w_i = w_0 \left(1 - \frac{r_i}{r_h}\right) \quad (38)$$

Function of the frustum around the hinge is as below

$$w = w_i - \frac{w_i}{R - r_i} (r - r_i) = \frac{w_0(r_h - r_i)(R - r)}{r_h(R - r_i)} \quad r_i \leq r \leq R \quad (39)$$

The final shape function of the plate would be:

$$w_f = w_0 \left(1 - \frac{r}{R}\right) \quad (40)$$

For a conical profile, radial and circumferential curvatures and strains are as follow:

$$k_r = 0 \quad (41)$$

$$k_\theta = -\frac{w_0}{rR} \quad (42)$$

$$\varepsilon_r = \frac{1}{2} \left(\frac{dw}{dr}\right)^2 + zk_r, \quad (43)$$

$$\varepsilon_\theta = zk_\theta \quad (44)$$

where, considering Equation (41) and (43) would be

$$\varepsilon_r = \frac{1}{2} \left(\frac{dw}{dr}\right)^2 \quad (45)$$

## PLASTIC WORKS

Total plastic work includes the dissipated works of hinge at the support, shear force in the support, moving plastic

hinge and circumferential bending moment. Calculating these work components, it is possible to obtain the critical impulse for occurrence of the complete deformation and tearing. Here, there is no second deformation and it is assumed that exposed impulse will be more than the critical impulse, which causes rigid motion of the plate after severance.

When the hinge is at  $r_i$ , in order to obtain work of the radial membrane force, radial strain is calculated using Equations (36) to (45) as

$$\varepsilon_r = \frac{1}{2} \frac{w_0^2 (r_h - r_i)^2}{r_h^2 (R - r_i)^2} \quad (46)$$

The work of this force component is as follow:

$$E_{N_r} = 2\pi h \sigma_d \int_{r_i}^R r \varepsilon_r dr = \frac{1}{2} \frac{\pi h \sigma_d w_0^2 (r_h - r_i)^2 (R^2 - r_i^2)}{r_h^2 (R - r_i)^2} \quad (47)$$

At the end of deformation process that the hinge is at the center, the absorb energy by this force component would be

$$E_{N_r} = \frac{1}{2} \pi h \sigma_d w_0^2 \quad (48)$$

To evaluate the work of circumferential membrane force, the circumferential strain when the hinge is at  $r_i$ , is obtained as follows:

$$\varepsilon_\theta = \frac{zw_0(r_h - r_i)}{rr_h(R - r_i)} \quad (49)$$

Similarly, the work of this force component when the hinge is at  $r_i$  is as follow:

$$E_{N_\theta} = 4\pi \sigma_d \int_{r_i}^R \int_0^{\frac{h}{2}} r \varepsilon_\theta dr = \frac{1}{2} \frac{\pi \sigma_d w_0 (r_h - r_i) h^2}{r_h} \quad (50)$$

Similarly, the absorb energy by this force component will be

$$E_{N_\theta} = \frac{1}{2} \pi \sigma_d w_0 h^2 \quad (51)$$

Considering Equation (39), circumferential curvature in frustum around is obtained as

$$k_{\theta_i} = \frac{w_0(r_h - r_i)}{rr_h(R - r_i)} \quad (52)$$

Thus, the work of circumferential bending moment when the hinge is at  $r_i$ , will be obtain as follow:

$$E_{M_{\theta_i}} = 2\pi \int_{r_i}^R M_{\theta} k_{\theta_i} r dr = \frac{2\pi M_d w_0 (r_h - r_i)}{r_h} \tag{53}$$

At the end of process,  $r_i = 0$ , so the Equation (53) that represents the total work of circumferential bending moment would be as follow:

$$E_{M_{\theta}} = 2\pi M_d w_0 = \frac{\pi w_0 \sigma_d h^2}{2} \tag{54}$$

Bending moment in the edge area is reached to the yield limit. The plastic work done by circular plastic hinge at the support, neglecting the shear sliding, would be as

$$E_{M_s} = 2\pi R M_d \theta_f = 2\pi M_d w_0 \tag{55}$$

In a cone, the radial curvature is zero, so work of the radial bending moment would be zero. Work of the moving circular plastic hinge at the end of process could be obtained in the following form:

$$E_{M_h} = \int_{r_h}^0 2\pi r_i M_d \theta dr_i \tag{56}$$

which results as

$$E_{M_h} = \int_{r_h}^0 \frac{2\pi r_i M_d}{R - r_i} w_0 \left(1 - \frac{r_i}{r_h}\right) dr_i = -\frac{2\pi M_d w_0 \Psi}{r_h} \tag{57a}$$

with

$$\Psi = R(R - r_h) \left(\ln \frac{R}{R - r_h}\right) - \left(R - \frac{r_h}{2}\right) r_h. \tag{57b}$$

Now, total deformation plastic work can be obtained as follow:

$$E_p = E_{N_r} + E_{N_b} + E_{M_b} + E_{M_s} + E_{M_h} = \frac{1}{2} \pi \sigma_d w_0 h \left( \left(2 + \left(\frac{\Psi}{r_h}\right)\right) h + 2w_0 + h \right) \tag{58}$$

In a condition where the input impulse is more than critical impulse, the plastic work at the support would be

$$W_{supp} = E_{s_{h\theta}} + E_{M_s} = 2\pi R Q_d \Delta^3_{cr} + 2\pi M_d w_0 \tag{59}$$

In the presented equations,  $r_h$  is the initial position of the hinge, its amount depends on radius of charge and stand-off. Here, it is assuming that hinge position can be considered initially according to relation given by (Jones and Alves, 2010), as follow:

$$r_h = \frac{R}{v} \left( \sqrt{v^2 - 4v + 1} - 1 \right) \tag{60a}$$

$$v = \frac{R}{h} \tag{60b}$$

In fact, in the first mode of failure in which no rupture is happened, mid-point deflection of the plate will be obtain by equating equations (58) and input energy. But as mentioned before, by increasing the input impulse more than critical amount, the second mode will be happened and the plate would tear apart from the support. By reducing stand-off distance, the final profile tends to have a conical like shape. So, the following equation is presented for stand-off distance less than the plate radius (Gharababaei et al., 2010):

$$\frac{w_0}{h} = \frac{\sqrt{1 + \frac{4}{\lambda} \phi^2} - 1}{2(aJ_1(a))} \tag{62}$$

where  $a$  is 2.4048. For the materials listed in Table 1, the mid-point deflection thickness ratios versus imparted impulses are plotted in the Figures 15 to 17.

As expected, mid-point deflection thickness ratio for both thicknesses,  $h = 1.6$  and  $2 \text{ mm}$ , are approximately same, but the critical impulses for occurrence of the second failure mode are completely different. These values are computed by  $29.77$  and  $46.50 \text{ N.s}$  for  $h = 1.6$  and  $2 \text{ mm}$ , respectively. Therefore, thickness of plate has sensible effect on the initiating tearing of plate and deformation is not enough to predict failure. For the case of copper sheet deformation, maximum impulse for  $2 \text{ mm}$  plate is  $46.50 \text{ N.s}$  and for  $3 \text{ mm}$  is  $104.60 \text{ N.s}$ . For impulses more than these values, plate will tear apart from support and the second mode of failure is happened. In Figure 16 the mid-point deflection thickness ratio for the copper plate are plotted versus input impulse. Figure 17 shows the mid-point deflection thickness ratio versus input impulse for the aluminum sheets with thicknesses equal to  $2$  and  $3 \text{ mm}$ .

It is observed that the predictions for the mid-point deflections are more than experimental data. It may be because of the fact that, as mentioned previously, in the experiment process, the final shape is not a full cone and that there is some radial curvature.

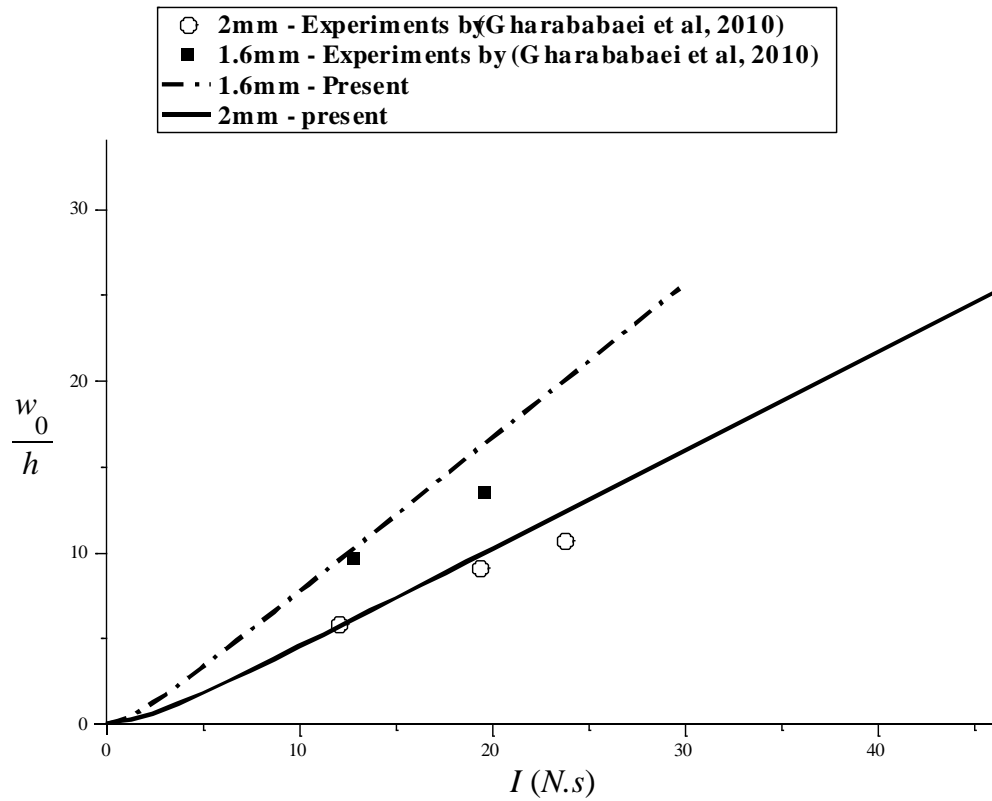


**Figure 15.** The mid-point deflection thickness ratios versus impulse for mild steel plate (1.6 and 2 mm thickness).

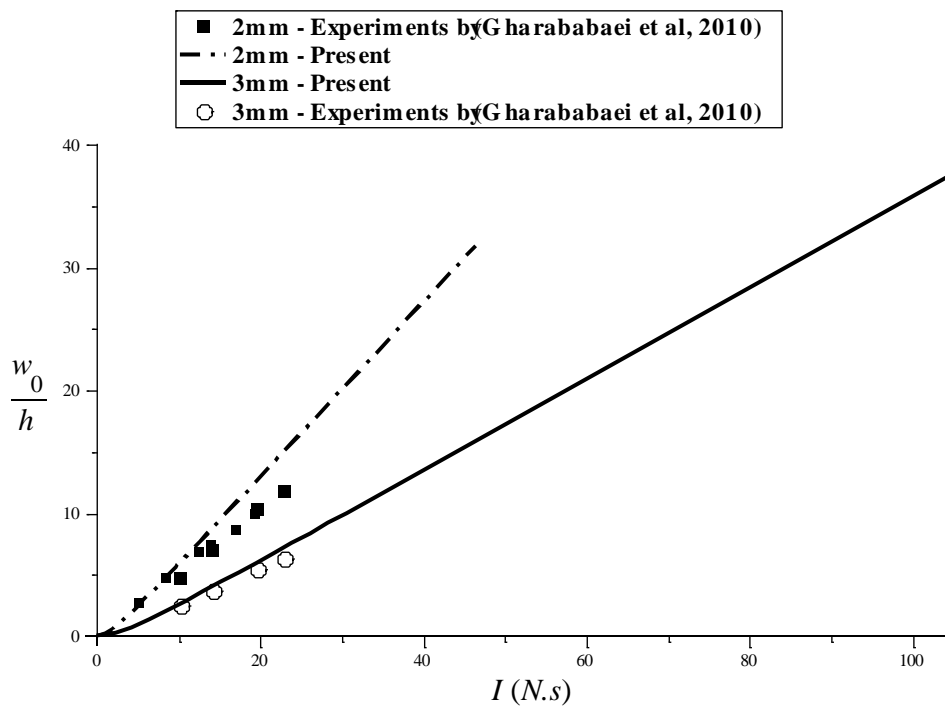


**Figure 16.** The mid-point deflection thickness ratios versus impulse for copper plate (2 and 3 mm thickness).

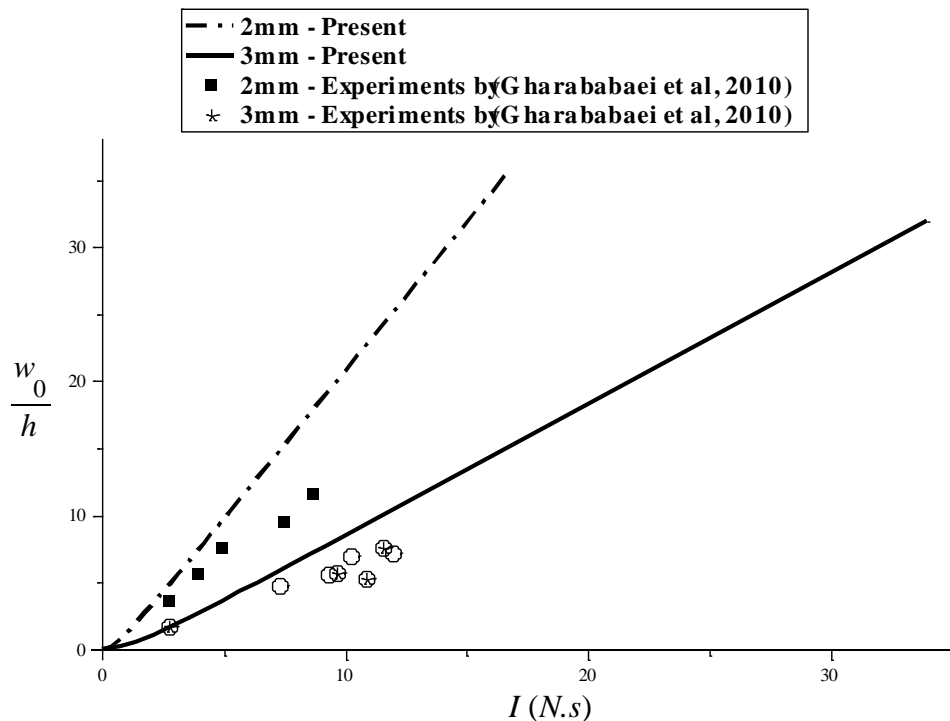


**Figure 17.** The mid-point deflection thickness ratio versus impulse for Aluminum plate (2 and 3 mm thickness).

A comparison between two approaches for yield lines (plastic hinges) are presented in Figure 18. As it is seen in this figure, residual velocity in the conical deformation scheme is more than the dome shape mechanism based on concept of multi-plastic hinge at the same loading condition. This is because of being more elements displacement in the dome shape deformation as compared to the conical shape at the same central deflections. The important point is that the residual velocities at the local failure had been produced differently by these models.

Although, analytical models can often predict final mid-point deflection relatively near real data (Gharababaei and Darvizeh, 2011, 2011; Gharababaei et al., 2010), these compatibilities are not enough to guarantee efficiency of the modeling for prediction of the failure procedure. In fact, these predictions must be accompanied by the velocity quantities, in particular, if the critical velocity is the basis of judgment about each model for stage after the tearing. This point has been delicately highlighted in previous experimental work (Teeling-Smith and Nurick, 1991).

## Conclusion

Using an effective approach for the limit analysis, behaviors of the circular metallic plates under impulsive

loads were investigated. At first, forming process of plate was considered by assuming several circular yield lines (hinges). Comparisons of obtained results with existing experimental data illustrated good compatibility. In some cases, present modeling predicted final displacement of plate more accurate than other proposed models. Simplifying a failure criterion, the energy absorbed in the boundaries was calculated. Also, the residual energy and velocity of plate after severance were determined. In addition, impulse limits for occurrences of the first and second failure modes were obtained.

In the first part of paper, a new deformation model was established on the concept of multi plastic hinges. In this model, several peripheral yield lines were formed. It was observed that by increasing these hinges lines, extracted results would be closer to the experimental data. Three different radial distributions of the hinges were investigated, individually. In the distribution type that hinges were closer together around of supports, results got convergent faster than others. This situation seems to be more convenient for plasticization in edge area.

Moreover, in the second part, an idealized deformation model was proposed by a moving circular hinge, which was responsible for deformation. Plate started to deform following movement style of hinge so that an idealized final shape was considered by a conical shape. The initial position of the hinge could be function of loading condition but here, an available relation was modified to

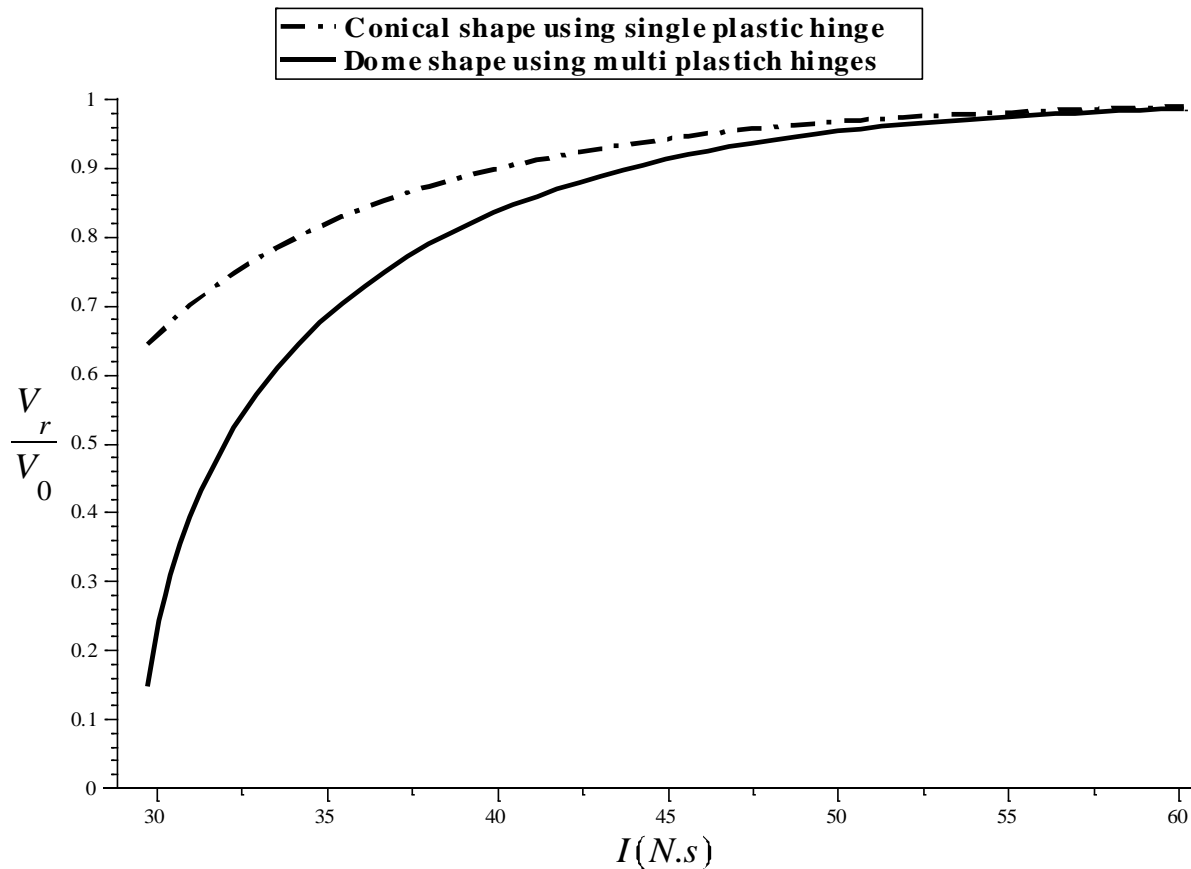


**Figure 18.** The Residual velocity initial velocity ratio versus input impulse for mild steel (1.6 mm).

complete model. The differences between results were because of different final shape considered here by a complete cone, while experimental data was showing the final shape else a complete cone.

It is concluded calculation of residual velocity in failure should be regarded with more precaution and accuracy in each straightforward analysis.

## REFERENCES

- Babaei H, Darvizeh A (2012). Analytical study of plastic deformation of clamped circular plates subjected to impulsive loading. *J. Mech. Mater. Struct.* 7(4):309-322.
- Balden VH, Nurick GN (2005). Numerical simulation of the post-failure motion of steel plates subjected to blast loading. *Int. J. Impact. Eng.* 32:14-34.
- Bodner SR, Symonds PS (1979). Experiments on viscoplastic response of circular plates to impulsive loading. *Int. J. Mech. Phys. Solids* 27:91-113.
- Gharababaei H, Darvizeh A (2010). Experimental and analytical investigation of large deformation of thin circular plates subjected to localized and uniform impulsive loading. *Mech. Based. Des. Struct. Mach.* 38(2):171-189.
- Gharababaei H, Darvizeh A (2011). Investigation into the Response of fully clamped circular Steel, Copper, and Aluminum Plates Subjected to Shock Loading. *Mech. Based. Des. Struct. Mach.* 39(4):507-526.
- Gharababaei H, Darvizeh A, Darvizeh M (2010). Analytical and experimental studies for deformation of circular plates subjected to blast loading. *J. Mech. Sci. Tech.* 24(9):1855-1864.
- Gupta NK, Nagesh (2007). Deformation and tearing of circular plates with varying support conditions under uniform impulsive loads. *Int. J. Impact. Eng.* 34:42-59.
- Jones N (1997). *Structural Impact*. Cambridge: Cambridge University Press.
- Jones N (2010). Inelastic response of structures due to large impact and blast loadings. *J. Strain Anal. Eng. Des.* 45(6):451-464.
- Jones N (2012). Impact loading of ductile rectangular plates. *Thin-Walled Struct.* 50:68-75.
- Jones N, Alves M (2010). Post-failure behavior of impulsively loaded circular plates. *Int. J. Mech. Sci.* 52:706-715.
- Jouri WS, Jones N (1988). The impact behaviour of aluminum alloy and mild steel double-shear specimens. *Int. J. Mech. Sci.* 30(3/4):153-172.
- Kobayashi S, Oh SI, Altan T (1989). *Metal forming and the finite – element method*. Oxford University Press.
- Lee YW, Wierzbicki T (2005a). Fracture prediction of thin plates under localized impulsive loading. Part I: dishing. *Int. J. Impact. Eng.* 31:1253-1276.
- Lee YW, Wierzbicki T (2005b). Fracture prediction of thin plates under localized impulsive loading. Part II: dicing and petalling. *Int. J. Impact. Eng.* 31:1277-1308.
- Menkes SB, Opat HJ (1973). Tearing and shear failures in explosively loaded clamped beams. *Exp. Mech.* 13:480-486.
- Nurick GN (1985). A new technique measure the deflection-time history of a structure subjected to high strain rates. *Int. J. Impact. Eng.* 3:17-26.

- Nurick GN, Gelman ME, Marshall NS (1996). Tearing of blast loaded plates with clamped boundary conditions. *Int. J. Impact. Eng.* 18(7-8):803-827.
- Nurick GN, Martin JB (1989). Deformations of thin plates subjected to impulsive loading - a review; Part I - Theoretical considerations. *Int. J. Impact. Eng.* 8(2):159-170.
- Shen WQ, Jones N (1993). Dynamic response and failure of fully clamped circular plates under impulsive loading. *Int. J. Impact. Eng.* 13:259-278.
- Symonds PS, Wierzbicki T (1979). Membrane mode solution for impulsively loaded circular plates. *J. Appl. Mech.* 46:58-64.
- Teeling-Smith RG, Nurick GN (1991). The deformation and tearing of thin circular plates subjective to impulsive loads. *Int. J. Impact. Eng.* 11(1):77-91.
- Ueda Y, Yao T (1982). The plastic node method of plastic analysis. *Comput. Method. Appl. M.* 34:1089-1104.
- Wen HM (1998). Deformation and tearing of clamped circular work-hardening plates under impulsive loading. *Int. J. Pres. Ves. Pip.* 75:67-73.
- Yu TX, Chen FL (2000). A further study of plastic shear failure of impulsively loaded clamped beams. *Int. J. Impact. Eng.* 24:613-629.
- Zajkani A, Darvizeh A, Darvizeh M (2012). Analytical modeling of high rate elasto-viscoplastic deformation of circular plates subjected to impulsive loads using pseudo-spectral collocation method. *J. Strain Anal. Eng. Des.* 48(2):126-149.
- Zajkani A, Sefidi SHR, Darvizeh A, Darvizeh M, Gharababaei H (2010). Mathematical modeling of large-amplitud dynamic-plastic behavior of circular plates subjected to impulsive loads. *J Mech.* 26(2):431-444.